Proposal of metal bellows-based fiber Bragg grating accelerometer

Jinghua Zhang (张敬花)*, Xueguang Qiao (乔学光), Manli Hu (忽满利), Zhongyao Feng (冯忠耀), Hong Gao (高 宏), Yang Yang (杨 扬), and Rui Zhou (周 锐)

Department of Physics, Northwest University of China, Xi'an 710069, China

**Corresponding author: 1982zhangjinghua@163.com*

Received January 24, 2011; accepted April 11, 2011; posted online June 30, 2011

A metal bellows-based fiber Bragg grating (FBG) accelerometer is proposed and experimentally demonstrated. The optical fiber (containing the FBG) is pre-tensioned, and the two ends of the optical fiber are fixed directly from the shell to the inertial mass. In this design, the FBG is uniformly tensioned to obtain a constant strain distribution over it. By employing this configuration, the FBG always has a sharp reflection characteristic with no broadening in its reflection spectrum during wavelength shifting. Dynamic vibration measurements show that the proposed FBG accelerometer has a wide frequency response range (5–110 Hz) and an extremely high sensitivity (548.7 pm/g). The two important indicators of FBG accelerometer can be tuned by the addition of mass to tailor the sensor performance to specific applications, identifying it as a good candidate for structural health monitoring.

OCIS codes: 060.2370, 230.1480, 050.2770.

doi: 10.3788/COL201109.090606.

Low-frequency vibration widely exists in mechanical devices and in large-scale construction structures[1−3]. Because the electromagnetism class accelerometer is presently mainly used to collect low-frequency vibration, some insufficiencies[4,5] naturally exist, for instance electromagnetic interference and being vulnerable to corrosion, thus affecting the application of electromagnetism class accelerometer in various fields. Fiber Bragg grating (FBG) sensor is a kind of optical fiber sensor that is extremely being developed rapidly at present[6−8] because of its advantages of small size, electromagnetic immunity, and being perfectly suited for long-term outdoor usage for highly corrosion resistant. FBG-based sensors have facilitated the research for the measurement of acceleration[9−11]. It can only make up for electromagnetic-type sensor in the application, thus the FBG accelerometer is of great significance.

A bellows-like accelerometer based on FBG is developed for acceleration measurement of large-scale engineering structures that may have low-frequency vibration. In this letter, a prototype FBG accelerometer is manufactured. It has high sensitivity for acceleration measurement at low frequency range. It is excited with an electromechanical shaker over a frequency band ranging from 1 to 200 Hz. The response of the FBG accelerometer is observed to be in good agreement with the applied signal. The accelerometer is identified as a good candidate for embedding in structural health monitoring applications.

The main body of the FBG-based accelerometer comprises the FBG sensing element and a spring mass configuration. The inertial mass (material: brass; weight: 20 g; through-hole diameter: 0.2 mm) is attached to one end of a metal bellows (material: beryllium bronze) and the other end is fixed to the shell. The external vibration introduces the acceleration change on the inertial mass, which subsequently induces the strain variation on the metal bellows. While the FBG sensing element is directly attached on the metal bellows, it will stretch or compress during the acceleration of the inertial mass; such strain or pressure applied on the grating will cause a change in the reflected wavelength, which can be converted theoretically to strain[12]. The schematic diagram of the accelerometer is shown in Fig. 1. The assembly process of the FBG-based accelerometer is presented in Fig. 2.

As shown in Fig. 1, the sensing element is a FBG, with length of 10 mm and 1 532.4 nm central wavelength, which passes through a hole drilled in the inertial mass; the hole is large enough for the fiber to have no contact with the inertial mass. A certain lever of tension stress is ensured by pre-tensioning the fiber with the Bragg grating and keeping the two side points fixed; if the FBG is fixed with glue in the whole setup, it is very difficult to control the uniformity of the thickness of the glue. When the force acts on the substrate, the FBG will sustain force, which is different. Consequently, the uniform grating spacing will be changed, which would induce the chip spectrum. In our experiment, with the approach of keeping the two side points fixed and the middle area being vacant, the pulling force at both ends acts uniformly on the FBG, and the change in grating

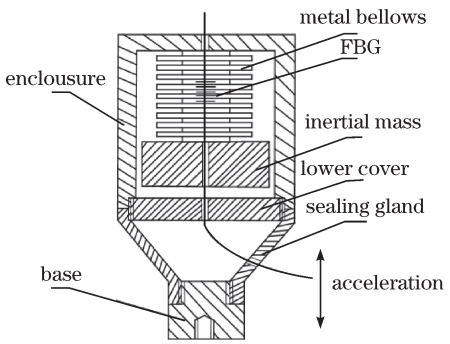

Fig. 1. Schematic diagram of FBG-based accelerometer.

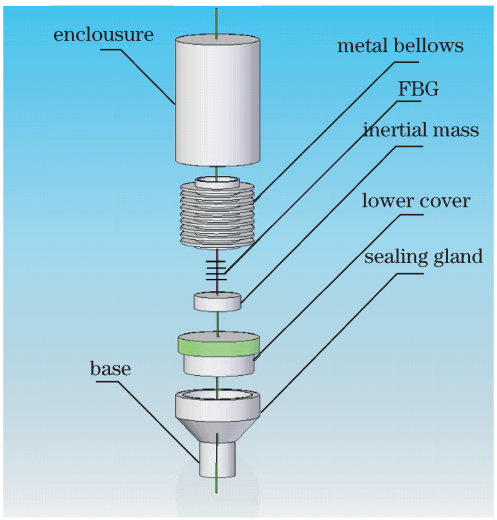

Fig. 2. Assembly drawing of FBG-based accelerometer.

spacing is the same. In this way, the chip effect can be effectively avoided.

Once the FBG-based accelerometer is subjected to a vertical acceleration, defined as a, the generated force applied to the sensor system is ma, where m is the sum of the inertial mass. A vertical acceleration produces an inertial displacement along the vertical axis (Fig. 1). The axial deformation ΔL of the FBG can be related to the acceleration a, as follows[13]:

$$\Delta L = \frac{F}{K_{\text{bellows}}} = \frac{ma}{K_{\text{bellows}}}, \tag{1}$$

where K_{bellows} is the characteristic elastic constant of a metal bellows given by $K_{\text{bellows}} = \frac{0.78ED_{\text{m}}h_0^3}{\left(\frac{t}{2}\right)^{0.5}H^{2.5}}\frac{D_{\text{m}}}{2d}$, where E is the Young modulus of the metal bellows; D_{m}, h_0, d, H, and t are the basic data of metal bellows, as shown in Table 1.

Table 1. Basic Data Sheet of Metal Bellows and the Dimensions of the Prototype

Parameters	Value
Internal Diameter (d)	15 mm
External Diameter (D)	27 mm
Average Diameter (D_{m})	21 mm
Wall Thickness (h_0)	0.12 mm
Corrugation Height (H)	3 mm
Corrugation Pitch (t)	2 mm
Young Modulus of the Material (E)	131×109 Nm^{-2}
Mass (m)	20 g
Central Wavelength of FBG	1 532.4 nm
Effective Length of the Optical Fiber (L)	30 mm
Rigidity K_{bellows}	1.44921×104 Nm^{-1}

Notes: 30 mm is the whole fiber that contains the FBG fixed from the shell to the inertial mass.

According to the mechanics of the materials theory[14], the axial strain ε of the FBG is described as

$$\varepsilon = \frac{\Delta L}{L} \tag{2}$$

where L is the effective length of the optical fiber.

The Bragg wavelength shift $\Delta\lambda_{\text{B}}$ of a segment of FBG at different positions has the following relationship with the axial strain ε if isothermal conditions are considered[15]:

$$\frac{\Delta\lambda_{\text{B}}}{\lambda_{\text{B}}} = (1 - P_{\text{e}})\varepsilon, \tag{3}$$

where λ_{B} is the strain-free Bragg wavelength of the FBG and $P_{\text{e}} \approx 0.22$ is the effective elastic-optic coefficient of the fiber.

From the above analysis, the wavelength shift of FBG is induced by the vertical vibration; therefore, the sensitivity coefficient S_{n} of the sensor is defined as the Bragg wavelength shift length under units exciting the acceleration. It can be derived by substituting Eqs. (1) and (2) into Eq. (3), which can be calculated as

$$S_{\text{n}} = \frac{\Delta\lambda_{\text{B}}}{a} = \frac{(1 - P_{\text{e}})m\lambda_{\text{B}}}{K_{\text{bellows}}L}. \tag{4}$$

According to the equation of the motion of the harmonic oscillator, the natural frequency f_{n} of the FBG accelerometer can be expressed as

$$f_{\text{n}} = \frac{1}{2\pi}\sqrt{\frac{K_{\text{bellows}}}{m}}. \tag{5}$$

In Table 1, the basic data sheet of metal bellows and the dimensions of the prototype are reported. Replacing them with the specific numbers given in this letter, the sensitivity coefficient and natural frequency of the FBG accelerometer are S_{n}=349.8 pm/g and f_{n} = 135.5 Hz, respectively.

From Eqs. (4) and (5), the sensitivity coefficient S_{n} and natural frequency f_{n} of the FBG accelerometer are related to the materials and geometry size of the metal bellows and the mass of m, respectively. Furthermore, sensitivity is inversely proportional to natural frequency. The FBG accelerometer is further optimized against various design parameters to realize an optimum response for real field structure health monitoring applications.

The experimental setup of a prototype FBG accelerometer consists of a vibration control system (console) including a signal generator, filter circuits, and power amplifier, and the exciter is used as the input in Fig. 3. The FBG accelerometer and a standard piezoelectric accelerometer are fixed on the same exciter actuator to guarantee that their vibrations are the same. The standard piezoelectric accelerometer is used for comparison in the experiment. The input signal is gained by the standard piezoelectric accelerometer; it is used for calibrating the FBG accelerometer. In a realistic experiment, the FBG accelerometer is installed in an environment where the temperature changes very slowly. In such environment, the wavelength shift of FBG is impacted by the temperature. However, in our experiment, the vibration

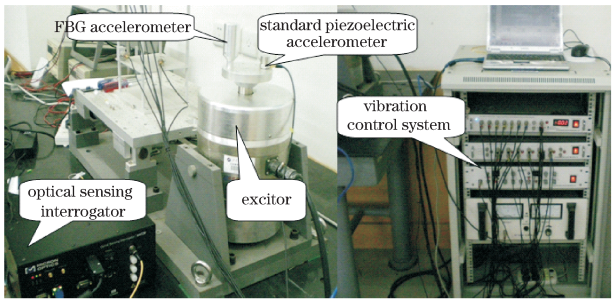

Fig. 3. Experimental setup of the acceleration-sensing system.

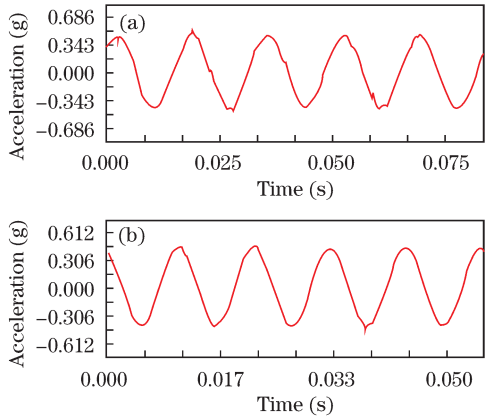

Fig. 4. Time domain traces of standard piezoelectric accelerometer with input frequencies of (a) 60 and (b) 90 Hz.

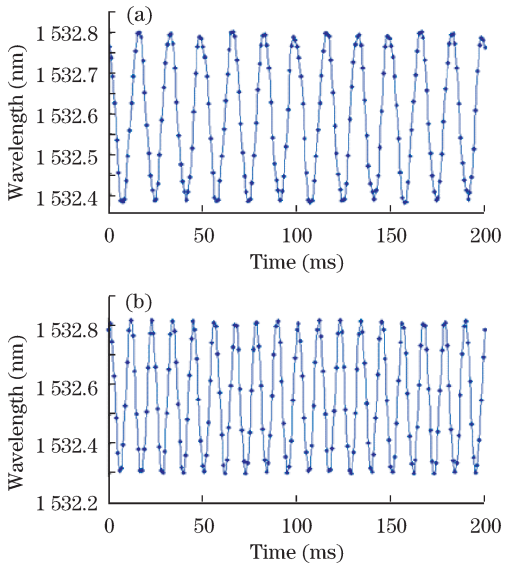

Fig. 5. Time domain traces of FBG accelerometer with input frequencies of (a) 60 and (b) 90 Hz.

frequency is at least dozens of hertzs. Therefore, the wavelength shift of FBG introduced by the temperature can be ignored. The shaker is used in all the following tests. A series of dynamic vibration measurements are taken to verify the dynamic characteristics of the FBG accelerometer.

During the experiment, the input is a sine wave with various input frequency, while the acceleration is 0.4 g. The output signals of both the compact metal bellows FBG accelerometer and the reference piezoelectric accelerometer are monitored simultaneously. Figures 4−6 show the time domain traces and frequency spectra of the acceleration recorded by the FBG accelerometer and the reference piezoelectric accelerometer under various input frequencies. The response of the FBG accelerometer is observed to be in good agreement with the applied signal; the experimental results show that the FBG accelerometer is capable of monitoring acceleration. The experiment indicates that the time domain response of the FBG-based accelerometer (Fig. 5) displays clear phase delay compared with the standard piezoelectric accelerometer (Fig. 4), which is in agreement with the theory. Some high-frequency interferences found in the frequency domain analysis graphics (Fig. 6) are mainly caused by the noise during the process of photoelectric conversion and circuit amplification, but they do not influence the accuracy of the results.

It is very important for the accelerometer to have a flat response over a range of resonance frequencies in its practical use. In the amplitude-frequency relationship test, diverse damping liquid is injected into the FBG-based accelerometer, and the amplitude-frequency characteristics of the FBG accelerometer with various damping is investigated. The experimental result is shown in Fig. 7. The FBG accelerometer is excited over a frequency band from 10 to 200 Hz, and the vibration acceleration value (approximately 1.6 m/s^2) is unchanged during the

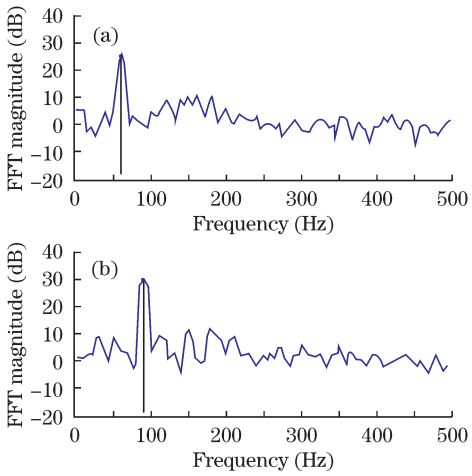

Fig. 6. Frequency spectra of FBG accelerometer with input frequencies of (a) 60 and (b) 90 Hz.

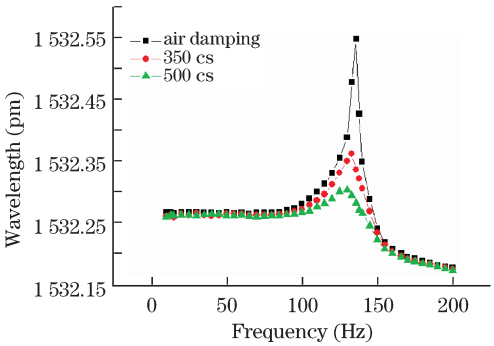

Fig. 7. Amplitude-frequency of FBG accelerometer with various damping.

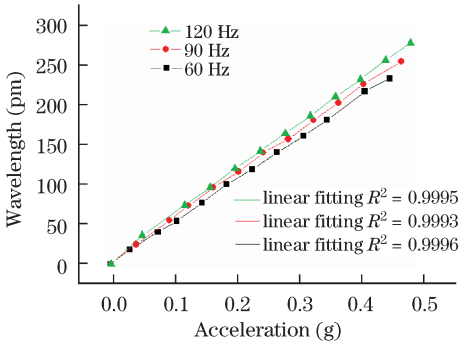

Fig. 8. Sensitivity and linearity of FBG accelerometer. R^2: linearity of linear fitting.

test process. The output signal of the wavelength variation of the FBG accelerometer can be recorded by an optical sensing interrogator. As can be seen from Fig. 5, the wavelength of the FBG is clearly diminishing and the range of measurement frequency becomes wider with the increase in the viscosity of the damping liquid. Figure 7 indicates that the natural frequency of the FBG-based accelerometer is 137 Hz.

The influence of frequency on the sensitivity of the accelerometer is investigated. The values of the input acceleration vary from 0 to 0.478 g, gained from the standard piezoelectric accelerometer. The wavelength shift of the FBG is detected by the optical sensing interrogator. The sensitivities of the FBG accelerometers for input frequencies of 60, 90, and 120 Hz are shown in Fig. 8. The sensitivity values under these frequencies are 325.9, 348.7, and 373.04 pm/g, respectively. The error is less than 5%, and the linearity of the accelerometer is good.

In conclusion, a metal bellows accelerometer based on the FBG is proposed. The results of a series of shake table tests show that the FBG accelerometer has good performance characteristics including the following: (i) broad range of flat response (works from 5 to 110 Hz); (ii) high sensitivity (about 548.7 pm/g) achieved with a large measurement range of 0.5 g; (iii) linearity of the accelerometer under different frequencies being superior to 99.93%; (iv) the possibility for natural frequency and sensitivity to be tuned by the addition of mass at the bottom of the metal bellows. For structural health monitoring of large-scale engineering structures, arrays of the FBG accelerometer should be provided.

This work was supported by the International S&T Cooperation Project of China by the MOST of China (No. 2009DFG13050), the National "863" Program of China (Nos. 2007AA06Z413 and 2009AA06Z203), the Key Scientific and Technological Research Project of Shaanxi Province (Nos. 20092KC01-19 and 2008ZDGC-14), and the National Natural Science Foundation of China (Nos. 60727004 and 61077060).

References

1. A. Mita and I. Yokoi, Proc. SPIE **4330,** 479 (2001).
2. P. Yan and T. Qaio, J. Vibration Measurement Diagnosis (in Chinese) **22,** 247 (2000).
3. P. F. C. Antunes, P. A. M. Almeida, J. L. Pinto, and P. S. B. Andre, in *Proceedings of Physics Teaching in Engineering Education PTEE 2007* (2007).
4. T. Hu, Y. Zhao, X. Li, J. Chen, and Z. Lü, Chin. Opt. Lett. **8,** 392 (2010).
5. T. A. Berkoff and A. D. Kersey, IEEE Photon. Technol. Lett. **8,** 1677 (1996).
6. K. Li and Z. Zhou, Chin. Opt. Lett. **7,** 191 (2009).
7. H. Dong, J. Wu, and G. Zhang, Chin. Opt. Lett. **7,** 23 (2009).
8. T. H. T. Chan, L. Yu, H. Y. Tam, Y. Q. Ni, S. Y. Liu, W. H. Chung, and L. K. Cheng, Eng. Struct. **28,** 648 (2006).
9. M. D. Todd, G. A. Johnson, B. A. Althouse, and S. T. Vohra, IEEE Photon. Technol. Lett. **10,** 1605(1998).
10. W. Zhou, X. Dong, Y. Jin, and C. Zhao, Proc. SPIE **7634,** 763413 (2009).
11. H. Y. Au, S. K. Khijwania, and H. Y. Tam, Proc. SPIE **7004,** 70042S (2008).
12. Y. Zhang, Z. Yin, B. Chen, and H. Cui, Proc. SPIE **5765,** 1112 (2005).
13. G. Gagliardi, M. Salza, P. Ferraro, P. De Natale, A. Di Maio, S. Carlino, G. De Natale, and E. Boschi, Meas. Sci. Technol. **19,** 085306 (2008).
14. E. J. Hearn, *Mechanics of Materials* (Antony Rowe, Eastbourne, 1997).
15. Z. Chen, "Investigation on the novel accelerometer based on the fiber grating" Master Thesis (in Chinese) (Xiamen University, 2009).